Environmental Science: Atmospheres

ROYAL SOCIETY OF CHEMISTRY

PAPER

View Article Online
View Journal

Cite this: DOI: 10.1039/d6ea00004e

Reduced U.S. methane emissions during the COVID-19 pandemic

Sergio Ibarra-Espinosa, †*[ab] Lei Hu,[b] Colin Harkins,[ac] Brian C. McDonald,[c] Scot M. Miller,[d] Youmi Oh,[ab] Lori Bruhwiler,[b] Colm Sweeney[b] and Arlyn Andrews[b]

The coronavirus disease 2019 (COVID-19) pandemic disrupted normal human activities worldwide, and mobility reductions resulted in reduced levels of air pollutants and greenhouse gases emissions. Here, we examine the impact of these disruptions on a potent greenhouse gas, methane (CH_4), over the U.S. In this study, we quantified CH_4 emissions from the contiguous U.S. between 2019 and 2021 by analyzing inverse modeling results derived from atmospheric measurements made at 35 sites across the country. Our estimates indicate emission reductions of −2.5 (±0.43) Tg year^{-1} CH_4 in 2020 and −2.9 (±1.63) Tg year^{-1} in 2021, relative to 2019. The respective percentage change was a −4.3 (−5.1 to −3.5) % reduction in 2020 and −4.8 (−8.3 to −0.7) % in 2021, relative to 2019. Combining with process-based inventory emission datasets, we found that this reduction was primarily due to decreased fossil fuel and agricultural emissions; however, record-breaking forest fires resulted in an increase of 0.4 (0.1 to 0.8) Tg year^{-1} in 2020–2019, equal to a 20 (3 to 46) % increase in CH_4 emissions from the western U.S.

Received 7th January 2026
Accepted 1st May 2026

DOI: 10.1039/d6ea00004e

rsc.li/esatmospheres

Environmental significance

This study leverages the COVID-19 pandemic as a unique "natural experiment" to assess the sensitivity of atmospheric monitoring systems to abrupt changes in anthropogenic activity. By applying high-resolution inverse modeling to atmospheric methane (CH_4) observations across the U.S., we detected and quantified subtle emission reductions in 2020 and 2021 that process-based inventories partly underestimated. Specifically, our results reveal that while fossil fuel reductions were consistent with drilling activity declines, agricultural emission reductions—likely driven by disruptions in the livestock sector—were more pronounced than reported in the EPA Greenhouse Gas Inventory. Furthermore, the analysis captures the opposing signal of record-breaking wildfire emissions in the Western U.S. These findings demonstrate the critical role of top–down atmospheric inversions in verifying bottom–up inventories and refining our understanding of how specific sectors drive regional methane budgets, a key step for designing effective climate mitigation policies.

Introduction

The Coronavirus disease 2019 (COVID-19) pandemic profoundly disrupted global socioeconomic activities and human behavior.[1,2] Between the first cases of infection in China in December 2019 and October 2023, there were more than 676 million registered cases and almost 7 million deaths.[3] Many governments implemented lockdowns and quarantines to limit spread of the virus.[4] Consequently, human mobility was reduced, corroborated by daily anonymized reports from internet companies using smartphones and other devices.[5,6] During that period, air quality improved in many cities worldwide.[7]

In this study, we investigated the impact of COVID-19 on U.S. emissions of CH_4, a potent greenhouse gas with a ∼11.8 year atmospheric lifetime and a Global Warming Potential of 27 to 30 over 100 years.[8] Its current atmospheric abundance contributes a total radiative forcing of 0.54 (0.43 to 0.65) W m^{-2} relative to 1750.[8] On average, between 2008 and 2017, global CH_4 emissions have been 577 (550–594) Tg year^{-1}, with the primary sources being agriculture, fossil fuel production and use, and wetlands.[9] The main sink of atmospheric CH_4 is the reaction with hydroxyl radicals (or OH).[10] Atmospheric mole fractions of CH_4 increased in the decades before 2000, were relatively stable between 1999 and 2006, and have since increased rapidly.[11–13] Some studies have proposed that the recent increases in global atmospheric CH_4 abundance are due to intensified emissions from microbial sources such as wetlands and agriculture, in combination with reduced atmospheric mole fractions of OH.[14–18]

CH_4 emission estimates for the U.S. show discrepancies across studies and inventories. For example, the U.S. Environmental Protection Agency Greenhouse Gas Inventory (USEPA-GHGI), a bottom–up inventory based on activity data and

[a]Cooperative Institute for Research in Environmental Sciences, University of Colorado-Boulder, Boulder, CO, USA. E-mail: sibarrae@umd.edu
[b]NOAA Global Monitoring Laboratory, Boulder, CO, USA
[c]NOAA Chemical Sciences Laboratory, Boulder, CO, USA
[d]Department of Environmental Health and Engineering, Whiting School of Engineering, Johns Hopkins University, Baltimore, MD 21218, USA
† Now at Cooperative Institute for Satellite Earth System Studies (CISESS)/Earth System Science Interdisciplinary Center (ESSIC), University of Maryland.

emission factors from various source categories, shows a small negative trend in total anthropogenic CH_4 emissions, with 33 Tg year^{-1} in 1990 and 29 Tg year^{-1} in 2019.[19] In 2021, the energy and agriculture sectors were reported to emit 11 Tg year^{-1} and 10 Tg year^{-1}, or 38% and 36% of total U.S. anthropogenic CH_4 emissions, respectively. Other studies using different approaches provide varying estimates. NOAA's CarbonTracker-CH4, an atmosphere-based inversion model that uses CH_4 and CH_4 isotope observations to constrain sectors, estimated 29 Tg year^{-1} fossil emissions in 2021 for the contiguous United States (CONUS).[20] A fuel-based inventory focusing on direct measurements and modeling specific to the oil and gas sector reported 15 Tg year^{-1} for oil and gas emissions in the CONUS in 2015.[21] For natural sources in the U.S., estimates also differ, ranging from 9.5 Tg year^{-1}, average 2010 to 2017,[22] 14.3 Tg year^{-1}, average 2008 to 2017,[9] to 12.5 Tg year^{-1}, average 2010 to 2019.[23] These variations underscore inconsistencies in the current understanding of U.S. CH_4 emissions, arising from uncertainties inherent in the different estimation methods.

The marked reduction in anthropogenic activity during the COVID-19 pandemic provided a unique opportunity to investigate its impact on emissions of key pollutants and greenhouse gases, such as CH_4. However, this area of research remains a complex area of study, evidenced by discrepancies in quantitative estimates across different analyses and scales. The EPA's GHGI reported that U.S. anthropogenic CH_4 emissions decreased by 0.6 Tg year^{-1} (2.1%) from 2019 to 2020 and by 1.3 Tg year^{-1} (4.3%) from 2019 to 2021.[19] In CarbonTracker-CH4, a near-zero change was found for the U.S. between 2019 and 2020 and a reduction of 2.2 Tg year^{-1} (−3.5%) was found by comparing 2019 and 2021.[20] Nevertheless, both estimates agree with the fact that there was a more substantial reduction in 2021 than in 2020,[24] using the satellite-based TROPOspheric Monitoring Instrument (TROPOMI) observations and a 4D-Var Integrated Forecasting System (4D-Var IFS), compared the first six months of 2020 with 2019 and found a global increase of 1.6%, and a 2.2% increase in the U.S. In California, aircraft measurements in 2020 revealed a 35% reduction relative to 2017 in CH_4 emissions from the oil and gas sector.[25] Here, we analyze U.S. CH_4 emissions from 2019 to 2021 derived from a high-resolution regional inverse modeling study.[26] We used the notation 2020–2019 and 2021–2019 to represent the anomaly period of the pandemic years, 2020 and 2021, *versus* the pre-pandemic year 2019. Using these atmospheric observation-based emission estimates, we investigate changes in U.S. national and regional CH_4 emissions during and after the COVID-19 pandemic relative to the pre-pandemic year of 2019. Then, we compare these changes with process-based inventories to improve the characterization of changes in CH_4 emissions during and after the COVID-19 pandemic.

Methods

U.S. CH_4 emissions derived from atmospheric observations

The observations used in this study are shown in SI Fig. S1 and S2 showing atmospheric CH_4 observations between 2019 and 2021 over the U.S., assimilated by.[26] Different from many national-scale CH_4 inversions over the U.S. (*e.g.*, 22, 27, 28),[26] simulated atmospheric transport at high resolution (10–12 km horizontally with 40–60 vertical levels), determined the error covariance matrices with an objective approach, and conducted an ensemble of analytical inversions with different considerations of background values and prior emissions. In this study, we analyzed the six inversion results from (ref. 26) that included three background and two prior emission estimates, incorporating OH loss by considering monthly climatological 3D OH concentrations. We aggregated the 1° × 1° × weekly posterior emissions from the inversions into national and regional emissions each year, as posterior national and regional emission estimates have much smaller uncertainties than grid-scale estimates. Posterior uncertainties of national and regional emissions from each inversion were calculated from the full posterior error covariance matrix that included cross correlations among grid cells.[27,28]

The presented uncertainties for the annual emissions below include two measures of uncertainty as described in (ref. 29). One is the analytical (internal) uncertainty that quantifies the random errors within a single inversion resulted from prior error covariance and model-data mismatch errors. This quantity reflects how well the atmospheric observations constrain emissions given a specific set of prior assumptions and background estimate. Hence, observational constraints should result in a decrease in uncertainty relative to the prior uncertainty. To characterize the features of our inversion, we define the external uncertainty as one standard deviation across the results of the six ensemble members. This metric captures the sensitivity of the methane flux estimates to variations in prior assumptions, background and transport model configurations. A narrow ensemble spread, therefore, increases confidence that our findings are robust and not an artifact of a single set of modeling choices.

The pandemic anomalies were calculated from the difference in annual CH_4 emissions between the pre-pandemic year 2019 and the pandemic years 2020 and 2021 for each of the six ensemble members. Our best estimate of the pandemic CH_4 anomalies discussed below were the mean anomaly among the six members and their one standard deviation as its uncertainty. To determine if the emission changes between the pre-pandemic (2019) and pandemic (2020, 2021) periods were statistically significant, we used *z*-scores for each ensemble member and its associated uncertainty, as shown in Fig. S5. The *z*-score quantifies the difference between the groups in units of standard deviation, where a larger absolute *z*-score and a corresponding *p*-value < 0.05 indicate a statistically significant difference.[30] In addition, we used the non-parametric Mann–Whitney *U* Test, appropriate for comparing two independent groups, in this case the ensemble group for each year and region, as shown in Table S1.

Estimates of U.S. natural and anthropogenic CH_4 emissions

To isolate the anthropogenic CH_4 signal from the atmospheric observation-based total net CH_4 emissions discussed above, we subtracted estimates of natural emissions from the

atmosphere-based top–down estimates. Natural emission estimates exhibit discrepancies among different products due to different data sources and methodologies. To account for this variability, we considered multiple datasets. Table 1 summarizes the 2019–2021 average values and standard deviations (representing interannual variability) of these natural emission components over the U.S., as used in this study. The natural emission estimates inputs for CarbonTracker-CH4,[31] derived from a combination of inventory data and process-based modeling, include: wetlands (16.3 ± 0.4 Tg year^{-1}), soil sink (−6.3 ± <0.1 Tg year^{-1}), termites (0.4 ± <0.1 Tg year^{-1}), wild animals (0.2 ± <0.1 Tg year^{-1}), and geological seeps (6.6 ± <0.1 Tg year^{-1}).[32–35] Although estimates of CH_4 emissions from geological seeps may contain a high bias,[36] this bias does not affect the estimates of interannual variabilities in natural or anthropogenic CH_4 emissions. Besides estimates from CarbonTracker-CH4, we also included wetland estimates calculated by (ref. 26) using the Kaplan model[37] (6.6 ± <0.1 Tg year^{-1} for 2006–2021, 1 × 1° resolution), and reported by (ref. 18) (Climate Research Units (CRU): 9.9 ± 0.1 Tg year^{-1}; Modern-Era Retrospective analysis for Research and Applications Version 2 (MERRA): 10.8 ± 0.2 Tg year^{-1} for 2001–2021, 0.5 × 0.5° resolution). Although there was a substantial difference in the magnitudes of wetland emissions among different products, their interannual variability between 2019–2021 is consistently small. The differences among these products were considered as the uncertainty in the U.S. natural CH_4 emissions and included in the overall uncertainty of our derived anthropogenic CH_4 emission estimates.

Auxiliary datasets

The estimated anthropogenic emissions from atmospheric inversions provide spatial information on the differences of U.S. CH_4 emissions during the COVID pandemic (2020–2021) relative to the pre-pandemic period (2019), but do not contain process information on the causes of differences. To investigate the processes that may have caused the differences in CH_4 emissions in 2020–2021 relative to 2019, we analyzed anthropogenic CH_4 emission inventories: the U.S. Environmental Protection Agency (EPA) Greenhouse Gas Inventory[19] and the NOAA CSL Fuel-based Oil and Gas (FOG) inventory.[21] For the U.S. EPA inventory, EPA collects inputs from federal and state agencies, as well as from industry and academic researchers. The FOG inventory was calculated following a bottom–up approach, with activity data at the facility level for sources such as drilling rigs, compressor stations, dehydrators and other equipment. The inventory was designed to estimate nitrogen oxides (NO_X) emissions[38] and expanded to CH_4 and non-methane volatile organic compounds (VOCs).[21] CH_4 and VOC emissions in FOG are estimated using the tracer–tracer ratios (CH_4/NO_X and VOC/CH_4) from measurements by the NOAA P3 aircraft during the Southeast Nexus (SENEX) 2013 and Shale Oil & Natural Gas Nexus (SONGNEX) 2015 field campaigns. For this study, the FOG inventory has been updated to separate drilling emissions from other production sources as well as to make monthly CH_4 emissions for the oil and gas production sector throughout the study time period. These updated emissions assume the same tracer–tracer ratios are applicable to both drilling and other production sources and also assume that these tracer–tracer ratios do not vary with time between 2015 (the year the ratios were developed for) and the COVID-19 study time period here (2019–2021). Both of these assumptions provide a basis for analysis in this study, as further airborne field campaigns to redetermine these values have not occurred. Satellite-derived estimates suggest that the CH_4 intensity from US oil and gas production has decreased with time,[39] while NO_X emissions have increased with production,[40] which future versions of FOG will incorporate. Therefore, the 2015 CH_4/NO_X ratio used to infer oil and gas CH_4 emissions during the COVID-19 period is likely an upper bound estimate. As cattle are a key contributor to agricultural CH_4 emissions, we also used the total cattle census data.[41] This report is a bi-annual publication by the National Agricultural Statistics Service (USDA/NASS) and distributed by Cornell University. This report provides a detailed inventory of all cattle and calves across the United States, by state, class (including beef and milk cows, and heifers held for breeding herd replacement), and number of operations. Lastly, we used emissions estimates from the Global Fire Emissions Database (GFED)[42] to understand CH_4 emissions from wildfires during our study period.

Results

U.S. annual total net CH_4 emissions in 2019, 2020, and 2021 were estimated to be 59.2 (±3.7, 1-sigma uncertainty), 56.7 (±3.7), and 56.3 (±3.3) Tgy^{-1}, respectively (Fig. S3). Considering 2019 as our reference year for the prepandemic period, there were reductions in the U.S. CH_4 emissions in 2020 and 2021

Table 1 Natural emissions products used in this study

Product	Sources	Timespan	Mean 2019–2021 (Tgy^{-1})	References
Carbon tracker – CH_4 priors	Wetlands	1984–2021	16.3 (±0.4)	33
	Soil sink		−6.3 (±< 0.1)	
	Termites		0.4 (±< 0.1)	34
	Wild animals		0.2 (±< 0.1)	32
	Geological seep		6.6 (±< 0.1)	35
Kaplan	Wetlands	2006–2021	6.6 (±< 0.1)	26
Zhang	Wetlands CRU	2001–2021	9.9 (±0.1)	18
	Wetlands MERRA	2001–2021	10.8 (±0.2)	

(Fig. 1a). In 2020, there was a decrease of −2.5 (±0.43) Tgy^{-1} or −4.3 (−5.1 to −3.5) %. In 2021, emissions were comparable to 2020 and below those in 2019 by −2.9 (±1.63) Tgy^{-1} or −4.8 (−8.3 to −0.7) %. The values in parentheses represent our best estimates of uncertainties, 1-sigma standard deviation of the differences in the changes among the six inversion members. Hence, uncertainties largely cancel out when calculating the interannual delta. Furthermore, average anomalies of priors (Fig. 1a) shows slight increases in CH_4 emissions in 2020–2021 relative to 2019, suggesting that the reduction in CH_4 emissions in the posterior estimates were derived from atmospheric observations. Additionally, Fig. S4 provides spatial maps comparing priors and optimized estimates. However, these changes represent the changes in the U.S. total net CH_4 emissions. In order to understand changes of CH_4 emissions related to anthropogenic activities, we need to separate natural emissions from the total net CH4 emissions. The differences between 2019 and 2020 or 2021 in the estimated natural CH_4 emissions (Fig. 1b), show little changes with the spread centered near zero, suggesting that the change in natural emissions during COVID-19 was insignificant in the U.S. The anthropogenic emissions calculated as optimized emissions from atmospheric observations minus natural emissions (Fig. 1c) follow a similar pattern. The estimated anthropogenic CH_4 emissions in 2020 was 2.6 (4.0 to 1.7) Tgy^{-1} or 5.6 (9.2 to 3.7) % lower than 2019. In 2021, anthropogenic CH_4 emissions were 2.9 (5.2 to 0.4) Tgy^{-1} or 6.1 (12.5 to 0.3) % lower than 2019.

To investigate the processes that may have caused the differences in CH_4 emissions in 2020–2021 relative to 2019, we analyzed process-based information from anthropogenic emission inventories. The U.S. EPA inventory-based emissions (Fig. 1d) are also lower in 2020 and 2021 compared to 2019, consistent with our finding, although smaller in magnitude. The 2020 reduction in the EPA inventory was −0.4 Tgy^{-1}, and, for 2021, it was −1.1 Tgy^{-1}, or −1.5% and −3.8%, respectively, relative to 2019. The EPA data suggest that this reduction was mainly caused by the energy sector, whose anomalies were −0.8 Tgy^{-1} and −1.1 Tgy^{-1}, or −6.7% and −9.7% for 2020 and 2021. The EPA-reported reductions of CH_4 emissions in the energy sector in 2020–2021 are also consistent with the change reported by the FOG inventory, but with lower magnitudes. The net decrease of CH_4 emissions in the oil and gas sector, estimated by the FOG inventory, is −1.1 Tgy^{-1} in 2020 and −1.6 Tgy^{-1} in 2021 relative to 2019 (Fig. 1e), representing −6.1% and −9.0% reductions. The reductions in FOG were dominated by reduced emissions from drilling, while emissions from other production activities were increased in 2020–2021. The CH4 emissions reduction associated with drilling was −2.8 Tgy^{-1} in 2020 and −1.9 Tgy^{-1} in 2021, similar to our optimized posterior anomalies. Besides reduction of CH_4 emissions in the energy sector, there were also likely reductions of CH_4 emissions from agriculture (Fig. 1g). Comparing U.S. Department of Agriculture (USDA) cattle inventory anomalies to EPA agriculture emission anomalies for 2020 and 2021, both relative to a 2019 baseline, reveals a consistent decreasing trend. USDA data show cattle inventory anomalies of −1.0% in 2020 and -1.2% in 2021 compared to 2019. The EPA's 2023 report indicates U.S. agriculture emission anomalies of 0.02 Tgy^{-1} (0.23%) in 2020 and −0.07 Tgy^{-1} (−0.76%) in 2021 relative to 2019. While the EPA's reported emission changes are smaller, particularly the slight increase in 2020, the decrease in both cattle inventory and overall agriculture emissions in 2021 relative to 2019 is consistent with the expected relationship between livestock numbers and a component of agricultural emissions, acknowledging that total agricultural emissions encompass various sources beyond just cattle. Wildfire CH_4 emissions shown in Fig. 1f) increased during this period, similarly to Land Use and Land Use Forestry (LULUF) in Fig. 1d), discussed in more detail in next section.

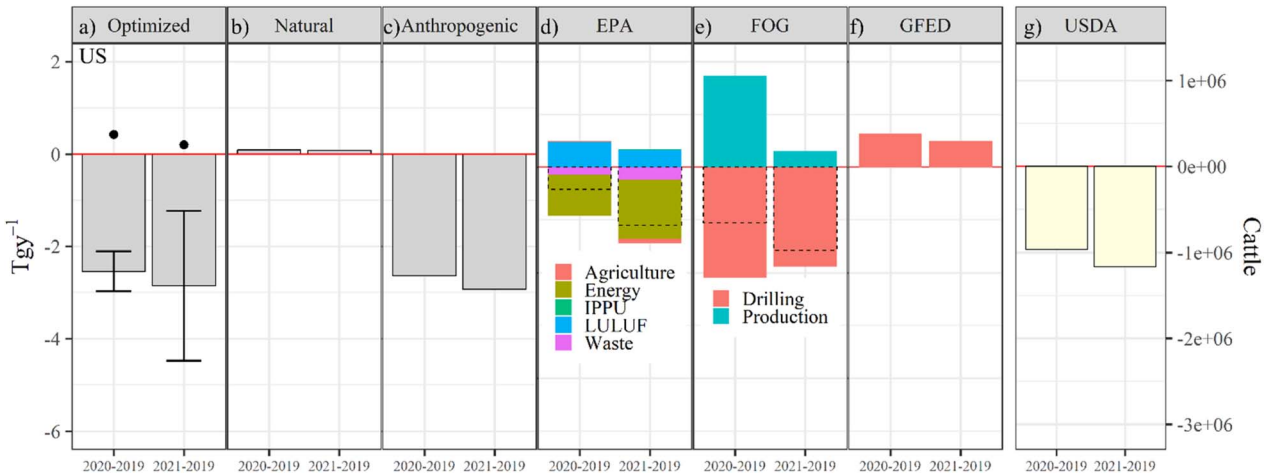

Fig. 1 Differences in 2020−2019 and 2021−2019 CH_4 emissions over the U.S. from the inversion for (a) net emissions, (b) the natural component, (c) the anthropogenic component, (d) from the U.S. EPA inventory,[19] (e) from the FOG oil and gas inventory,[21] and (f) global fire emissions database.[43] Error bars in panel (a) represent 1-sigma of the anomalies. Panel (g) shows the total number of cattle (heads) in the U.S.[41] EPA and FOG columns show the net results in dashed lines. The points represent the average anomaly for the priors.

The inversion system and spatial and temporal density of the measurements allow emissions to be derived on regional scales, which provide a spatial understanding of the changes during the COVID period. Hence, Fig. 2 shows the six regions considered in this study and Fig. 3 shows annual changes in total posterior emission changes by region. Consistent negative CH_4 emission anomalies observed across multiple datasets in the oil and gas-dominated Central South (CS) region point strongly to reduced drilling activity as the primary driver during the COVID period. We found negative anomalies in the optimized posterior fluxes, and given that the natural emissions in this region are insignificant, the anthropogenic component is very similar to the posterior values.

The negative anomalies in the U.S. EPA[19] are similar to our estimates and primarily arise from changes in the energy sector. The net anomaly in the FOG inventory also agrees with our results and those of the US. EPA.[19] Specifically, in the region CS, for the periods 2020–2019 and 2021–2019, we found reductions of -0.7 (± 0.31) Tgy^{-1} and -1.6 (± 0.51) Tgy^{-1}, in our posterior results. These changes are statistically significant after applying z-score test between the estimates of ensemble members, and Mann–Whitney *U* test, as shown in Fig. S5 and Table S1. In case of US EPA,[19] we found -0.6 Tgy^{-1} and -0.9 Tgy^{-1} for 2020–2019 and 2021–2019; and for FOG[21] -1.1 Tgy^{-1}. There are some reductions in cattle in the CS during these years. In this region, we also see a significant reduction in drilling and increment of methane emissions associated with oil and gas production. Indeed, a study found that during the pandemic, lower demand for oil and gas resulted in turned-off wells, reducing CH_4 emissions.[42] Other studies also found substantial CH_4 reductions in oil-dominated regions.[23,47] There are similarities between negative FOG emissions in the drilling sector and negative optimized estimates. Fig. S6 shows correlations with interval confidence between posterior emissions and FOG emissions by production and drilling. Here, we see that the region CS has significant correlations between posterior and drilling CH_4 emissions in 2020, corroborating that the main driver in reduced CH_4 emissions in 2020 was likely due to reduced drilling activities. The percentage change in the FOG-drilling inventory in 2020 and 2021, about 2019, was -46.6% and -31.4%, respectively, while the same change for the FOG-production sector was 15.1% and 2.7%. This is because the COVID lockdown resulted in fewer drilling activities and associated emissions, but the cause of production emissions increase is unclear. The total change was -6.1% from 2019 to 2020 and -9.0% from 2019 to 2021.

The Central North (CN) region exhibited substantial negative anomalies in the U.S. CH_4 emissions during the COVID period, representing one of the largest regional changes (Fig. 3). Specifically, for the periods 2020–2019 and 2021–2019, we found reductions of -3.4 (± 0.62) Tgy^{-1} and -3.3 (± 0.69) Tgy^{-1}, in our posterior results (see Fig. S5 and Table S1). The FOG shows negative anomalies for both periods, and production showed a slight increase in 2020–2019 and a reduction in 2021–2019. Even though these anomalies agree with the emission decrease in our results, they do not explain the higher magnitude of the changes found in our study. The EPA shows slight negative anomalies, which also are not consistent with the values we found. According to the U.S. EPA Greenhouse Gas Inventory report,[19] 70% of the CH_4 agricultural emissions come from enteric fermentation. Furthermore, among the agricultural categories (field burning of agricultural residues, enteric fermentation, manure management, and rice cultivation) only enteric fermentation exhibited strong and negative anomalies (Fig. S7), with a stronger anomaly in 2021 than 2020, similar to our results. Also, from the enteric fermentation sub-sector in the inventory,[19] beef cattle are responsible for 71% of the totals for 2021 and show a more significant negative anomaly than other animals, as shown in Fig. S8 SI, which is consistent with the anomalies presented by the U.S. EPA, but our findings suggest a potential under-representation. The methodology for the agriculture sector is Tier 2 of IPCC.[8] For the enteric fermentation, they use the Cattle Enteric Fermentation Model (CEFM), as shown in the Common Reporting Format (CRF) Source Category 3A.[48] This methodology uses estimates of cattle populations by animal type and state, as shown in table A-126, Annex 3, greenhouse gases report in the US.[48] Research has shown that 3-nitrooxypropanol (3-NOP), included in ruminants' diets, reduces methane emissions by about 30%.[49,50] However, 3-NOP (BovaerTM) was approved by the Food and Drug Administration just in 2024,[51] well after the period discussed here. Therefore, changes in the diet is not the cause to the reduction we observed at CN. During COVID-19 and the associated lockdowns, the livestock sector was particularly impacted because of a shortage of animal feed and health resources, workers, and a decrease in purchasing power.[52] Also, sharp decreases in meat, milk, and egg production have been documented during this period, which is explained by mobility restrictions of workers, including veterinary services, among others.[53] A map of the anomalies in livestock can be seen in Fig. S9. Furthermore, posterior emissions derived by multiple independent atmospheric inversions, *i.e.*, from ref. 26 CarbonTracker-CH4, Copernicus Atmosphere Monitoring Service, and[54] (Fig. S9 in ref. 26) in the CN region are higher than EPA inventory estimates, suggesting likely underestimation of agricultural emissions, and therefore reductions in agricultural emissions, by the EPA inventory.

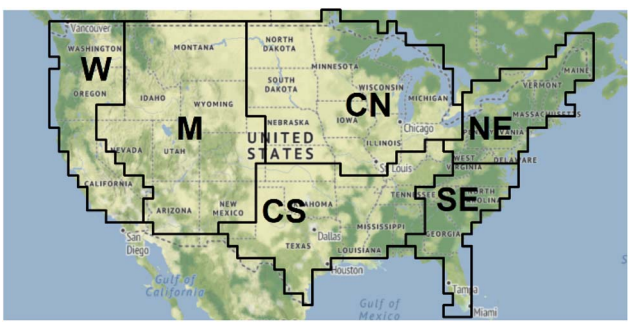

Fig. 2 Regions in the U.S.: northeast (NE), southeast (SE), central north (CN), central south (CS), mountain (M), west (W), as defined by (ref. 44). The figure was generated using R package ggmap[45] and ggplot2.[46]

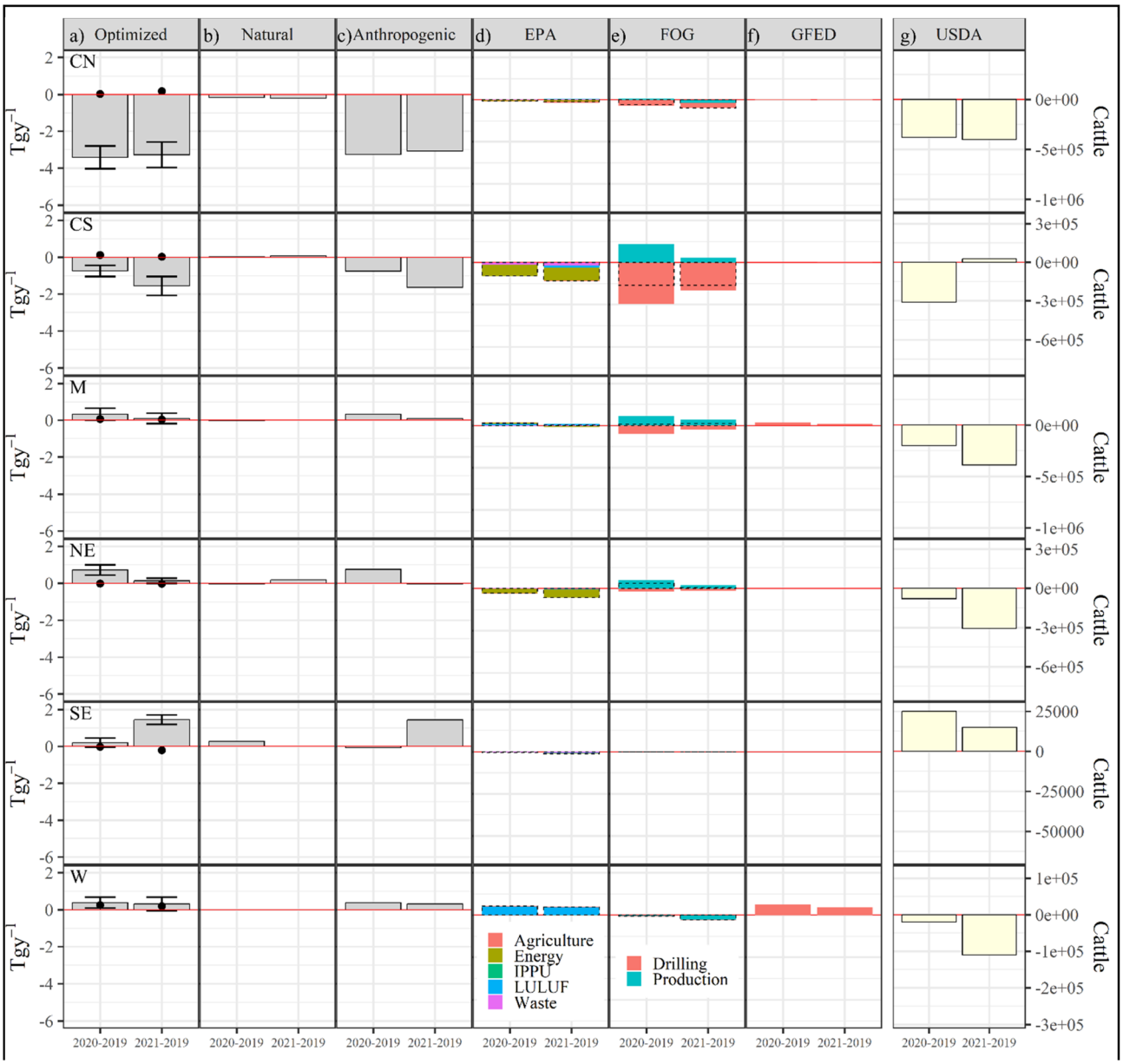

Fig. 3 Difference 2020–2019 and 2021–2019 in CH4 emissions over the US Tgy^{-1}, by regions in the US north east (NE), south east (SE), central north (CN), central south (CS), mountain (M), west (W), as defined by ref. 44 (a) year, (b) natural component, (c) anthropogenic component, (d) from U.S. EPA inventory,[19] (e) by the FOG oil and gas inventory,[21] and (f) Global Fire Emissions Database,[43] and (g) by the total number of cattle (heads) in the US.[41] Error bars in panel (a) represent 1-sigma of the anomalies. The points represent the average anomaly for the priors.

In the other regions, the anomalies had smaller magnitudes. In the North East (NE) region, there is only a significant increment of emissions for 2020–2019 (see also Fig. S5 and Table S1) and not 2021–2019, which agrees with production in FOG and US EPA showing small negative anomalies. The posterior anomalies in the South East (SE) region were only significant for 2021–2019 and not 2020–2019. Coincidentally, the cattle also showed a small increase of around 20 thousand heads. Since the SE region is a primarily sub-tropical region with high precipitation and humidity levels, natural emissions may play a more pivotal role here. The natural anomaly for 2020–2019 is significant for this region. Wetlands are an important source of natural CH_4 emissions,[9,16] and over the US, the southeast has a high density of this source. Our model captures the natural variability since the optimized posterior values agree with the natural anomalies derived independently, as shown in Fig. 2, panel (b) for the difference 2021–2019 in the region NE.

In the Mountain (M) region, our posterior total emission anomalies were +0.3 (±0.33) Tgy^{-1} for 2020 relative to 2019 and +0.1 (±0.28) Tgy^{-1} for 2021 relative to 2019. Nevertheless, the anomaly was not significant after checking scores and Mann–Whitney *U* test (p.value > 0.05) in Fig. S5 and Table S1, respectively. For comparison, US EPA inventory anomalies for the same periods were +0.11 Tgy^{-1} and +0.02 Tgy^{-1}, primarily

attributed to the LULUF sector. The GFED fire emissions dataset also indicated positive anomalies of +0.14 Tgy^{-1} and +0.09 Tgy^{-1} for 2020–2019 and 2021–2019, respectively. A slight negative anomaly in cattle was also observed in Fig. 3g.

In the West (W) region, our analysis reveals positive posterior anomalies of +0.4 (±0.29) Tgy^{-1} (2020–2019) and +0.3 (±0.37) Tgy^{-1} (2021–2019). These results align well with[19] inventory anomalies derived from the LULUF sector, reported as +0.4 Tgy^{-1} for both periods. Furthermore, the change was significant only for the period 2020–2019, also corroborated by the *z*-scores and Mann–Whitney *U* test Fig. S5 and Table S1. While the baseline LULUF sector emissions (per EPA definitions) are dominated by sources like flooded land remaining flooded (FLRF, 58.4%), which exhibit relatively stable emissions, our results indicate the observed positive anomaly in this region is driven primarily by Forest Fires (Fig. S10). This aligns with Forest Fires constituting 31.4% of baseline LULUF. California displayed the most significant state-level positive anomaly (Fig. S11), consistent with the record number of large fires in 2020 propagated by severe drought.[55] Therefore, our optimized fluxes effectively capture the influence of wildfire activity on CH_4 emissions, corroborating inventory trends.[19] Further, GFED biomass burning anomalies for the W region were substantial at 0.49 Tgy^{-1} (2020–2019) and 0.37 Tgy^{-1} (2021–2019). Indeed, the annual time series from GFED confirms that 2020 saw record-breaking wildfire emissions, particularly impacting the M and W regions in Fig. S12 and S13.

To investigate the influence of natural emissions further, we calculated the anthropogenic anomalies at 1-degree resolution by subtracting the natural emissions from our posterior emissions. As shown in Fig. S14, we then compared these anthropogenic anomalies with the posterior anomalies. The strong correlation observed suggests that the posterior emissions are primarily driven by the anthropogenic component, allowing us to focus on the posterior results for further analysis. No statistical differences and high correlations were inferred after applying Mann–Whitney U and correlation tests between total optimized and anthropogenic components, as shown in panels (c) and (f).

Even though[19] considered CH_4 losses related to its reactions with OH, the OH field considered were monthly climatological values that do not contain interannual variability. Studies found that atmospheric OH concentration was reduced globally and over regions like the US during the 2020 pandemic period, largely due to decreased NO_X emissions.[17] Globally, tropospheric OH concentrations decreased by 1.6 ± 0.2% relative to 2019, a reduction that could explain 53 ± 10% of the coincident increase in global atmospheric methane abundance in 2020.[17] Regional methane emission estimates are sensitive to interannually varying OH fields.[56] Over the U.S., the tropospheric OH reduction was approximately 5% at maximum due to pandemic-related NO_X emission decrease.[57] This reduction in OH has implications for methane budget calculations. For example, if less OH is present in the atmosphere, the atmospheric lifetime of CH_4 becomes longer. This increased lifetime enhances the contribution of background CH_4 arriving from remote regions to the concentrations observed at a measurement site and smaller concentration enhancements would be attributable to emissions. For instance, assuming a linear sensitivity to the pandemic-related 5% reduction in tropospheric OH to our 2020 posterior estimate of 56.7 Tgy^{-1} could increase the reported reduction of −2.5 Tgy^{-1} to −2.8 (2.6 to 3.0) Tgy^{-1}. This further supports our results as a conservative estimate of the pandemic's impact. Therefore, if reduction in OH was considered in ref. 26, a slightly larger reduction of CH_4 emission would be expected to be derived.

While our regional inversion[26] used a monthly climatological OH field, we now explicitly acknowledge that a global drop in OH during 2020–2021, driven by reduced NO_X and CO emissions, likely explained a dominant portion of the global methane surge.[11,12] Our finding of reduced U.S. fossil fuel emissions (particularly in the Central South) aligns with latest isotopic evidence showing that the record global surge in 2020–2022 was driven almost entirely by microbial sources, while fossil fuel emissions remained stable or declined in many regions.[14,15]

Discussion and conclusion

This study demonstrates that through a high resolution inversion approach that subtle changes (decreases) in emissions can be detected and provide valuable perspective relative to inventory estimates. Our results suggest percentage changes from 2019 to 2020 of −4.3 (−5.1 to −0.4) % and 2021 of −4.8 (−8.3 to −0.7) %, indicating reductions of methane emissions during the COVID pandemic in 2020–2021 relative to the prepandemic period in 2019. The reduction in CH_4 emissions was primarily driven by reduced anthropogenic activities during the COVID-19 pandemic. Natural anomalies, based on independent data sources used in this study, were insignificant in the U.S. and most regions. The energy sector, which significantly decreased drilling in the oil and gas industry in the Central South region, was a key contributor to the reduction of U.S CH_4 emissions in 2020 and 2021. While agricultural inventory-based estimates suggest a decrease in emissions, particularly from livestock, our study suggests the impact in this sector may be underestimated in the EPA's greenhouse gas emission inventory. We found that our model captured the impact of wildfire with the agreement between our results and positive anomalies in the EPA inventory in the West. The COVID-19 pandemic served as a natural experiment, allowing our study to document the impact of changes in key anthropogenic activities, particularly in oil and gas drilling and agriculture, on U.S. CH_4 emissions. These insights improve our understanding of drivers of variability of CH_4 emission during and after the COVID-19 pandemic.

Author contributions

SIE: formal analysis, visualization, writing – original draft, methodology, software. LH: conceptualization, funding acquisition, project administration, supervision, methodology, formal analysis, writing – review & editing. SIE, LH, CH, BM, YO, LB, SM, AA, CS: formal analysis, data curation, investigation, writing – review & editing.

Conflicts of interest

There are no conflicts to declare.

Data availability

Posterior CH_4 emissions estimated from this analysis are available at https://doi.org/10.15138/zmd2-cy30 as published by (ref. 26). NOAA's CH_4 data is publicly available and can be downloaded from https://gml.noaa.gov/dv/data/. For other questions related to data used or produced from this paper, please contact the corresponding author: Dr Sergio Ibarra-Espinosa (sibarrae@umd.edu).

Supplementary information (SI): assimilated methane monitoring network (aircraft and surface sites); regional optimization summaries for total, natural, and anthropogenic emissions alongside 2020 and 2021 anomalies; statistical evaluations (z-scores and Mann–Whitney U tests) of the regional inversions; and sector-specific data covering fossil oil and gas activity, agriculture, and biomass burning. See DOI: https://doi.org/10.1039/d6ea00004e.

Acknowledgements

This project is funded by the NOAA Climate Program Office AC4 and COM programs (NA21OAR4310233/NA21OAR4310234). This research was supported by the NOAA cooperative agreement NA22OAR4320151. We thank Stephen Montzka, John Miller, and Kathryn McKain for their scientific input on this analysis and paper. We also thank Kenneth Schuldt and Kirk Thoning for programming support. We thank the numerous technical and scientific staff at NOAA GML and CIRES and site partners for providing the atmospheric measurement data.

References

1 M. Ciotti, M. Ciccozzi, A. Terrinoni, W. C. Jiang, C. B. Wang and S. Bernardini, The COVID-19 pandemic, *Crit. Rev. Clin. Lab Sci.*, 2020, **57**(6), 365–388, DOI: 10.1080/10408363.2020.1783198.

2 A. Schuchat, Public health response to the initiation and spread of pandemic COVID-19 in the United States, February 24–April 21, 2020, *MMWR (Morb. Mortal. Wkly. Rep.)*, 2020, **69**, 551–556, DOI: 10.15585/mmwr.mm6918e2.

3 E. Dong, H. Du and L. Gardner, An interactive web-based dashboard to track COVID-19 in real time, *Lancet Infect. Dis.*, 2020, **20**(5), 533–534, DOI: 10.1016/S1473-3099(20)30120-1.

4 J. Cohen and K. Kupferschmidt, *Countries Test Tactics in 'war'against COVID-19*, DOI: 10.1126/science.367.6484.1287.

5 L. Alessandretti, What human mobility data tell us about COVID-19 spread, *Nat. Rev. Phys.*, 2022, **4**(1), 12–13, DOI: 10.1038/s42254-021-00407-1.

6 S. Ibarra-Espinosa, E. D. de Freitas, K. Ropkins, F. Dominici and A. Rehbein, Negative-Binomial and quasi-poisson regressions between COVID-19, mobility and environment in São Paulo, Brazil, *Environ. Res.*, 2022, **204**, 112369, DOI: 10.1016/j.envres.2021.112369.

7 R. S. Sokhi, V. Singh, X. Querol, S. Finardi, A. C. Targino, M. de Fatima Andrade, R. Pavlovic, R. M. Garland, J. Massagué, S. Kong and A. Baklanov, A global observational analysis to understand changes in air quality during exceptionally low anthropogenic emission conditions, *Environ. Int.*, 2021, **157**, 106818, DOI: 10.1016/j.envint.2021.106818.

8 Intergovernmental Panel on Climate Change (IPCC). *Climate Change 2021 - the Physical Science Basis: Working Group I Contribution to the Sixth Assessment Report of the Intergovernmental Panel on Climate Change*, Cambridge University Press, 2023.

9 M. Saunois, A. R. Stavert, B. Poulter, P. Bousquet, J. G. Canadell, R. B. Jackson, P. A. Raymond, E. J. Dlugokencky, S. Houweling, P. K. Patra and P. Ciais, The global methane budget 2000–2017, *Earth Syst. Sci. Data Discuss.*, 2019, **2019**, 1–36, DOI: 10.5194/essd-12-1561-2020.

10 Z. Qu, D. J. Jacob, L. Shen, X. Lu, Y. Zhang, T. R. Scarpelli, H. Nesser, M. P. Sulprizio, J. D. Maasakkers, A. A. Bloom and J. R. Worden, Global distribution of methane emissions: a comparative inverse analysis of observations from the TROPOMI and GOSAT satellite instruments, *Atmos. Chem. Phys.*, 2021, **21**(18), 14159–14175, DOI: 10.5194/acp-21-14159-2021.

11 P. Ciais, Y. Zhu, Y. Cai, X. Lan, S. E. Michel, B. Zheng, Y. Zhao, D. A. Hauglustaine, X. Lin, Y. Zhang and S. Sun, Why methane surged in the atmosphere during the early 2020s, *Science*, 2026, **391**(6785), eadx8262.

12 E. G. Nisbet and M. R. Manning, What is causing the methane surge?, *Science*, 2026, **391**(6785), 556–557.

13 X. Lan, E. G. Nisbet, E. J. Dlugokencky and S. E. Michel, What do we know about the global methane budget? Results from four decades of atmospheric CH4 observations and the way forward, *Philos. Trans. R. Soc. A Math. Phys. Eng. Sci.*, 2021, **379**(2210), 20200440.

14 B. Riddell-Young, S. E. Michel, X. Lan, P. Tans, T. Röckmann, B. Dasgupta, Y. Oh, L. M. Bruhwiler, R. Fujita, T. Umezawa and S. Morimoto, Microbial driver of 2006–2023 CH4 growth indicated by trends in atmospheric δD–CH4 and δ13C–CH4, *Proc. Natl. Acad. Sci. U. S. A.*, 2025, **122**(50), e2516543122.

15 S. E. Michel, X. Lan, J. Miller, P. Tans, J. R. Clark, H. Schaefer, P. Sperlich, G. Brailsford, S. Morimoto, H. Moossen and J. Li, Rapid shift in methane carbon isotopes suggests microbial emissions drove record high atmospheric methane growth in 2020–2022, *Proc. Natl. Acad. Sci. U. S. A.*, 2024, **121**(44), e2411212121.

16 Y. Oh, Q. Zhuang, L. R. Welp, L. Liu, X. Lan, S. Basu, E. J. Dlugokencky, L. Bruhwiler, J. B. Miller, S. E. Michel and S. Schwietzke, Improved global wetland carbon isotopic signatures support post-2006 microbial methane emission increase, *Commun. Earth Environ.*, 2022, **3**(1), 159, DOI: 10.1038/s43247-022-00488-5.

17 S. Peng, X. Lin, R. L. Thompson, Y. Xi, G. Liu, D. Hauglustaine, X. Lan, B. Poulter, M. Ramonet,

M. Saunois and Y. Yin, Wetland emission and atmospheric sink changes explain methane growth in 2020, *Nature*, 2022, **612**(7940), 477–482, DOI: 10.1038/s41586-022-05447-w.

18 Z. Zhang, B. Poulter, A. F. Feldman, Q. Ying, P. Ciais, S. Peng and X. Li, Recent intensification of wetland methane feedback, *Nat. Clim. Change*, 2023, **13**(5), 430–433, DOI: 10.1038/s41558-023-01629-0.

19 US Environmental Protection Agency (US EPA). Greenhouse gas inventory data explorer; 2023. https://cfpub.epa.gov/ghgdata/inventoryexplorer/.

20 Y. Oh, L. Bruhwiler, X. Lan, K. Schuldt and *et al. CarbonTracker CH4 2025*, 2025, DOI: 10.25925/hxks-v755.

21 C. B. Francoeur, B. C. McDonald, J. B. Gilman, K. J. Zarzana, B. Dix, S. S. Brown, J. A. de Gouw, G. J. Frost, M. Li, S. A. McKeen and J. Peischl, Quantifying methane and ozone precursor emissions from oil and gas production regions across the contiguous US, *Environ. Sci. Technol.*, 2021, **55**(13), 9129–9139, DOI: 10.1021/acs.est.0c07352.

22 X. Lu, D. J. Jacob, H. Wang, J. D. Maasakkers, Y. Zhang, T. R. Scarpelli, L. Shen, Z. Qu, M. P. Sulprizio, H. Nesser and A. A. Bloom, Methane emissions in the United States, Canada, and Mexico: evaluation of national methane emission inventories and 2010–2017 sectoral trends by inverse analysis of in situ (GLOBALVIEWplus CH 4 ObsPack) and satellite (GOSAT) atmospheric observations, *Atmos. Chem. Phys.*, 2022, **22**(1), 395–418, DOI: 10.5194/acp-22-395-2022.

23 M. Saunois, A. Martinez, B. Poulter, Z. Zhang, P. A. Raymond, P. Regnier, J. G. Canadell, R. B. Jackson, P. K. Patra, P. Bousquet and P. Ciais, Global methane budget 2000–2020, *Earth Syst. Sci. Data*, 2025, **17**(5), 1873–1958, DOI: 10.5194/essd-17-1873-2025.

24 J. McNorton, N. Bousserez, A. Agustí-Panareda, G. Balsamo, L. Cantarello, R. Engelen, V. Huijnen, A. Inness, Z. Kipling, M. Parrington and R. Ribas, Quantification of methane emissions from hotspots and during COVID-19 using a global atmospheric inversion, *Atmos. Chem. Phys.*, 2022, **22**(9), 5961–5981, DOI: 10.5194/acp-22-5961-2022.

25 A. K. Thorpe, E. A. Kort, D. H. Cusworth, A. K. Ayasse, B. D. Bue, V. Yadav, D. R. Thompson, C. Frankenberg, J. Herner, M. Falk and R. O. Green, Methane emissions decline from reduced oil, natural gas, and refinery production during COVID-19, *Environ. Res. Commun.*, 2023, **5**(2), 021006, DOI: 10.1088/2515-7620/acb945.

26 L. Hu, A. E. Andrews, S. A. Montzka, S. M. Miller, L. Bruhwiler, Y. Oh, C. Sweeney, J. B. Miller, K. McKain, S. Ibarra Espinosa and K. Davis, An unexpected seasonal cycle in US oil and gas methane emissions, *Environ. Sci. Technol.*, 2025, **59**(20), 9968–9979, DOI: 10.1021/acs.est.4c14090.

27 A. J. Turner, D. J. Jacob, K. J. Wecht, J. D. Maasakkers, E. Lundgren, A. E. Andrews, S. C. Biraud, H. Boesch, K. W. Bowman, N. M. Deutscher and M. K. Dubey, Estimating global and North American methane emissions with high spatial resolution using GOSAT satellite data, *Atmos. Chem. Phys.*, 2015, **15**(12), 7049–7069, DOI: 10.5194/acp-15-7049-2015.

28 H. Nesser, D. J. Jacob, J. D. Maasakkers, A. Lorente, Z. Chen, X. Lu, L. Shen, Z. Qu, M. P. Sulprizio, M. Winter and S. Ma, High-resolution US methane emissions inferred from an inversion of 2019 TROPOMI satellite data: contributions from individual states, urban areas, and landfills, *Atmos. Chem. Phys.*, 2024, **24**(8), 5069–5091, DOI: 10.5194/acp-24-5069-2024.

29 L. Hu, D. Ottinger, S. Bogle, S. A. Montzka, P. L. DeCola, E. Dlugokencky, A. Andrews, K. Thoning, C. Sweeney, G. Dutton and L. Aepli, Declining, seasonal-varying emissions of sulfur hexafluoride from the United States, *Atmos. Chem. Phys.*, 2023, **23**(2), 1437–1448, DOI: 10.5194/acp-23-1437-2023.

30 R Core Team, *R: A Language and Environment for Statistical Computing*, R Foundation for Statistical Computing, Vienna, Austria, 2024, https://www.R-project.org/.

31 Y. Oh, L. Bruhwiler, X. Lan, S. Basu, K. Schuldt, K. Thoning and *et al.*, *CarbonTracker CH4 2023*, NOAA Global Monitoring Laboratory, 2023, DOI: 10.25925/40JT-QD67.

32 S. Houweling, T. Kaminski, F. Dentener, J. Lelieveld and M. Heimann, Inverse modeling of methane sources and sinks using the adjoint of a global transport model, *J. Geophys. Res. Atmos.*, 1999, **104**(D21), 26137–26160, DOI: 10.1029/1999JD900428.

33 L. Liu, Q. Zhuang, Y. Oh, N. J. Shurpali, S. Kim and B. Poulter, Uncertainty quantification of global net methane emissions from terrestrial ecosystems using a mechanistically based biogeochemistry model, *J. Geophys. Res. Biogeosci.*, 2020, **125**(6), e2019JG005428, DOI: 10.1029/2019JG005428.

34 M. G. Sanderson, Biomass of termites and their emissions of methane and carbon dioxide: A global database, *Global Biogeochem. Cycles*, 1996, **10**(4), 543–557, DOI: 10.1029/96GB01893.

35 G. Etiope, G. Ciotoli, S. Schwietzke and M. Schoell, Gridded maps of geological methane emissions and their isotopic signature, *Earth Syst. Sci. Data*, 2019, **11**(1), 1–22, DOI: 10.5194/essd-11-1-2019.

36 K. R. Hall, T. S. Weber, M. P. Stock, M. L. Buursink, H. Piao, M. Zhu, K. M. Walter Anthony and V. V. Petrenko, New measurements indicate that natural geologic methane emissions from microseepage in the Michigan Basin are likely negligible, *Elem. Sci. Anth.*, 2026, **14**(1), 00058.

37 C. A. Pickett-Heaps, D. J. Jacob, K. J. Wecht, E. A. Kort, S. C. Wofsy, G. S. Diskin, D. E. Worthy, J. O. Kaplan, I. Bey and J. Drevet, Magnitude and seasonality of wetland methane emissions from the Hudson Bay Lowlands (Canada), *Atmos. Chem. Phys.*, 2011, **11**(8), 3773–3779.

38 A. M. Gorchov Negron, B. C. McDonald, S. A. McKeen, J. Peischl, R. Ahmadov, J. A. de Gouw, G. J. Frost, M. G. Hastings, I. B. Pollack, T. B. Ryerson and C. Thompson, Development of a fuel-based oil and gas inventory of nitrogen oxides emissions, *Environ. Sci. Technol.*, 2018, **52**(17), 10175–10185, DOI: 10.1021/acs.est.8b01799.

39 X. Lu, D. J. Jacob, Y. Zhang, L. Shen, M. P. Sulprizio, J. D. Maasakkers, D. J. Varon, Z. Qu, Z. Chen, B. Hmiel and

R. J. Parker, Observation-derived 2010-2019 trends in methane emissions and intensities from US oil and gas fields tied to activity metrics, *Proc. Natl. Acad. Sci. U. S. A.*, 2023, **120**(17), e2217900120, DOI: 10.1073/pnas.2217900120.

40 B. Dix, J. de Bruin, E. Roosenbrand, T. Vlemmix, C. Francoeur, A. Gorchov-Negron, B. McDonald, M. Zhizhin, C. Elvidge, P. Veefkind and P. Levelt, Nitrogen oxide emissions from US oil and gas production: recent trends and source attribution, *Geophys. Res. Lett.*, 2020, **47**(1), e2019GL085866, DOI: 10.1029/2019GL085866.

41 US Department of Agriculture (USDA). National Agricultural Statistics Service (NASS), Agricultural Statistics Board, 2024, https://usda.library.cornell.edu/concern/publications/h702q636h.

42 A. Townsend-Small and J. Hoschouer, Direct measurements from shut-in and other abandoned wells in the Permian Basin of Texas indicate some wells are a major source of methane emissions and produced water, *Environ. Res. Lett.*, 2021, **16**(5), 054081, DOI: 10.1088/1748-9326/abf1a6.

43 D. van Wees, G. R. van der Werf, J. T. Randerson, B. M. Rogers, Y. Chen, S. Veraverbeke, L. Giglio and D. C. Morton, Global biomass burning fuel consumption and emissions at 500 m spatial resolution based on the Global Fire Emissions Database (GFED), *Geosci. Model Dev.*, 2022, **15**(22), 8411–8437, DOI: 10.5194/gmd-15-8411-2022.

44 L. Hu, S. A. Montzka, J. B. Miller, A. E. Andrews, S. J. Lehman, B. R. Miller, K. Thoning, C. Sweeney, H. Chen, D. S. Godwin and K. Masarie, US emissions of HFC-134a derived for 2008–2012 from an extensive flask-air sampling network, *J. Geophys. Res. Atmos.*, 2015, **120**(2), 801–825, DOI: 10.1002/2014JD022619.

45 D. Kahle, H. Wickham. ggmap: Spatial Visualization with ggplot2. https://journal.r-project.org/archive/2013-1/kahle-wickham.pdf.

46 H. Wickham, *Data analysis. ggplot2: elegant graphics for data analysis*, Springer international publishing, Cham, 2016, 9, pp. 189–201.

47 D. R. Lyon, B. Hmiel, R. Gautam, M. Omara, K. Roberts, Z. R. Barkley, K. J. David, N. L. Miles, V. C. Monteiro, S. J. Richardson and S. Conley, Concurrent variation in oil and gas methane emissions and oil price during the COVID-19 pandemic, *Atmos. Chem. Phys. Discuss.*, 2020, **2020**, 1–43, DOI: 10.5194/acp-21-6605-2021.

48 US Environmental Protection Agency (US EPA), Inventory of U.S. greenhouse gas emissions and sinks: 1990-2021; 3.10. Methodology for estimating CH4 emissions from enteric fermentation, 2023, https://www.epa.gov/system/files/documents/2023-04/US-GHG-Inventory-2023-Annex-3-Additional-Source-or-Sink-Categories-Part-B.pdf.

49 A. N. Hristov, A. Melgar, D. Wasson and C. Arndt, Symposium review: Effective nutritional strategies to mitigate enteric methane in dairy cattle, *J. Dairy Sci.*, 2022, **105**(10), 8543–8557, DOI: 10.3168/jds.2022-21861.

50 E. Kebreab, A. Bannink, E. M. Pressman, N. Walker, A. Karagiannis, S. van Gastelen and J. Dijkstra, A meta-analysis of effects of 3-nitrooxypropanol on methane production, yield, and intensity in dairy cattle, *J. Dairy Sci.*, 2023, **106**(2), 927–936, DOI: 10.3168/jds.2022-22162.

51 Ohio Dairy Industry Resources Center (ODIRC). 3-NOP (BovaerTM) Receives FDA Approval. Ohio State University Extension, 2025, https://dairy.osu.edu/newsletter/buckeye-dairy-news/volume-26-issue-3/3-nop-bovaer%E2%84%A2-receives-fda-approval.

52 N. M. Hashem, A. González-Bulnes and A. J. Rodriguez-Morales, Animal welfare and livestock supply chain sustainability under the COVID-19 outbreak: An overview, *Front. Vet. Sci.*, 2020, **7**, 582528, DOI: 10.3389/fvets.2020.582528.

53 M. T. Rahman, M. S. Islam, A. A. Shehata, S. Basiouni, H. M. Hafez, E. I. Azhar, A. F. Khafaga, F. Bovera and Y. A. Attia, Influence of COVID-19 on the sustainability of livestock performance and welfare on a global scale, *Trop. Anim. Health Prod.*, 2022, **54**(5), 309, DOI: 10.1007/s11250-022-03307-4.

54 S. M. Miller, S. C. Wofsy, A. M. Michalak, E. A. Kort, A. E. Andrews, S. C. Biraud, E. J. Dlugokencky, J. Eluszkiewicz, M. L. Fischer, G. Janssens-Maenhout and B. R. Miller, Anthropogenic emissions of methane in the United States, *Proc. Natl. Acad. Sci. U. S. A.*, 2013, **110**(50), 20018–20022, DOI: 10.1073/pnas.1314392110.

55 S. Li and T. Banerjee, Spatial and temporal pattern of wildfires in California from 2000 to 2019, *Sci. Rep.*, 2021, **11**(1), 8779, DOI: 10.1038/s41598-021-88342-w.

56 D. A. Belikov, P. K. Patra and N. Saitoh, Hydroxyl interannual variability impacts estimation of regional methane emissions, *J. Geophys. Res. Atmos.*, 2026, **131**(4), e2025JD044457.

57 J. He, C. Harkins, K. O'Dell, M. Li, C. Francoeur, K. C. Aikin, S. Anenberg, B. Baker, S. S. Brown, M. M. Coggon and G. J. Frost, COVID-19 perturbation on US air quality and human health impact assessment, *PNAS Nexus*, 2023, **3**(1), pgad483, DOI: 10.1093/pnasnexus/pgad483.

